Electronic Supplementary Material (ESI) for Physical Chemistry Chemical Physics.

Supplementary information for the manuscript "Ab-initio design of light absorption through silver atomic clusters decoration of TiO_2"

María Pilar de Lara-Castells,[*,†] Carlos Cabrillo,[‡] David Micha,[¶] Alexander O. Mitrushchenkov,[§] and Tijo Vazhappilly[‖]

Instituto de Física Fundamental, C.S.I.C., Serrano 123, E-28006 Madrid, Spain, Instituto de Estructura de la Materia, C.S.I.C., Serrano 123, E-28006 Madrid, Spain, Quantum Theory Project, Departments of Chemistry and Physics, University of Florida, 32661-8435, United States, Université Paris-Est, Laboratoire Modélisation et Simulation Multi Echelle, MSME UMR 8208 CNRS, 5 bd Descartes, 77454 Marne-la-Vallée, France, and Theoretical Chemistry Section, Bhabha Atomic Research Centre, Mumbai 400085, India

E-mail: Pilar.deLara.Castells@csic.es

In the first section of this supplementary information, we present the optimized structures of bare Ag_3 and Ag_5 clusters. In Section S2, the $Ag/TiO_2(110)$ and Xe/TiO_2 interaction potentials are compared. A comparison of interaction energies obtained with two different samplings of the

[*]To whom correspondence should be addressed

[†]Instituto de Física Fundamental, C.S.I.C., Serrano 123, E-28006 Madrid, Spain

[‡]Instituto de Estructura de la Materia, C.S.I.C., Serrano 123, E-28006 Madrid, Spain

[¶]Quantum Theory Project, Departments of Chemistry and Physics, University of Florida, 32661-8435, United States

[§]Université Paris-Est, Laboratoire Modélisation et Simulation Multi Echelle, MSME UMR 8208 CNRS, 5 bd Descartes, 77454 Marne-la-Vallée, France

[‖]Theoretical Chemistry Section, Bhabha Atomic Research Centre, Mumbai 400085, India

Brillouin zone is also presented in Section S2. Finally, Section S3 presents complementary results on the $Ag_2/TiO_2(110)$ interaction.

Contents

S1 Optimizing the geometries of bare Ag_3 and Ag_5 clusters

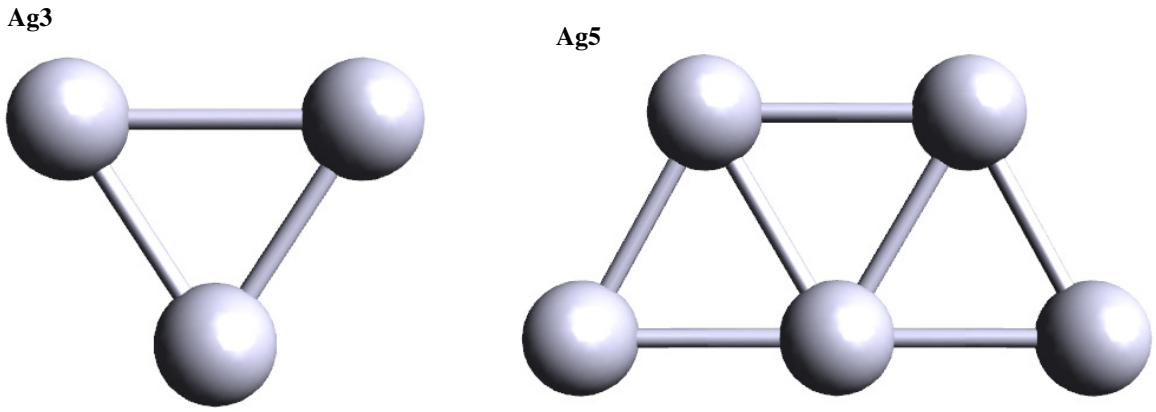

Figure S1: Optimized geometries of bare Ag_3 and Ag_5 clusters.

The geometries of bare Ag_3 and Ag_5 clusters were optimized at second-order Möller-Plesset perturbation theory (MP2) level using the def2-QZVPP[1] basis set. For this purpose, the ORCA program system[2] has been used (version 4.0.1.2). As can be seen in Figure S1, triangular (Ag_3) and planar trapezoidal (Ag_5) geometries were obtained, agreeing well with with experimental observations.[3] A bipyramidal Ag_5 structure was found to be 194 meV higher in energy at MP2 level. These geometries were reoptimized using the PBE-D3(BJ) approach and the same def2-QZVPP basis set. The Ag-Ag relative distances, d_{Ag-Ag}, are presented in Table S1. It can be observed that the lengths of the Ag-Ag bonds are longer using the PBE-D3(BJ) approach. The comparison of the Ag_2 bond length with the available experimentally determined value[4] (2.531 Å) indicates that the MP2-based d_{Ag-Ag} distances are underestimated (by ca. 0.05 Å for the Ag_2 cluster) while those calculated with the PBE-D3(BJ)-based scheme are sligthly overestimated (by ca. 0.03 Å for the Ag_2 cluster). Overall, these results indicate that the PBE-D3(BJ) approach provides sensible predictions of optimized Ag_n structures.

Table S1: Relative Ag-Ag distances, $d_{\mathrm{Ag-Ag}}$, in the optimized geometries of bare Ag_2, Ag_3 and Ag_5 clusters (see also Figure S1).

	$d_{\mathrm{Ag-Ag}}$, Å		
Cluster	Ag_2	Ag_3	Ag_5
MP2	2.48	2.55	2.62
PBE-D3(BJ)	2.56	2.59	2.68
Experiment[4]	2.53	–	–

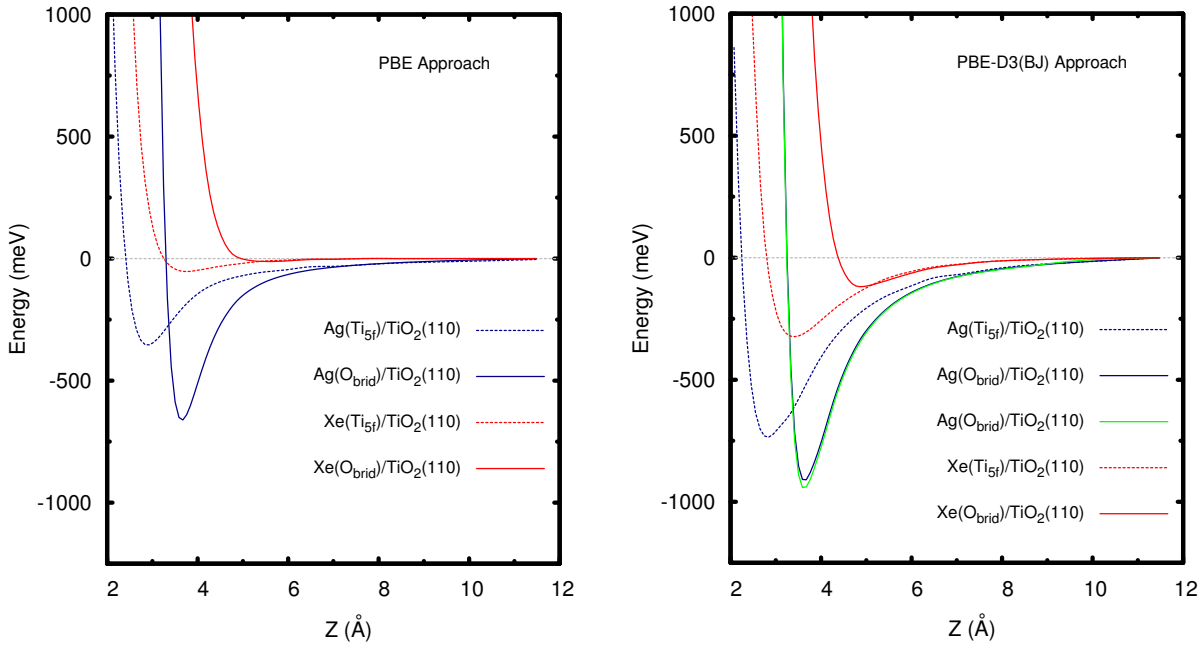

Figure S2: Comparison of $Ag/TiO_2(110)$ and $Xe/TiO_2(110)$ interaction energies using the PBE-D3(BJ) scheme (right-hand panel) and the vdW-uncorrected PBE approach (left-hand panel). The Xe and Ag atoms are located on top of either the five-fold coordinated Ti_{5f} atom (Ti_{5f} site, dashed line) or the bridging oxygen atom O_{brid} (O_{brid} site, full line). Z (in Å) stands for the distance between the Ag and Xe atom and the five-fold coordinated Ti_{5f} atom along the surface normal direction. Potential energy curves shown in red and blue were calculated using a $5\times5\times1$ Monkhorst-Pack[5] k-point mesh while that shown in green was obtained with the Brillouin zone sampled at the Γ point only.

S2 Comparing the Ag/TiO_2(110) and Xe/TiO_2(110) interactions

In this section, we compare the Ag/TiO_2(110) and Xe/TiO_2(110) interactions. The same computational set-up described in the main manuscript was followed for the periodic calculations. However, a $5\times5\times1$ Monkhorst-Pack[5] k-point mesh was also used in the present case. Relevantly, as can be seen in Figure S2, the potential energy curve estimated with the Brillouin zone sampled at the Γ point only is hard to be distinguished from that calculated a $5\times5\times1$ Monkhorst-Pack[5] k-point mesh. This outcome confirms the adequacy of the computational set-up. i.e., involving the sampling at the Γ point only.

The interaction of noble-gas atoms with solid surfaces are stereotypical dispersion-dominated interaction problems. Contrarily, attractive dispersionless energy contributions are expected to play a relevant role for the open-shell Ag/TiO_2(110) interaction. As can be observed in Figure S2, the Xe/TiO_2(110) interaction becomes significantly attractive when the D3(BJ) dispersion correction is added (see right-hand panel) while the well-depth values are very small without including it (see left-hand panel). As discussed in previous works (see, e.g., Refs. 6,7), the preferential adsorption site for noble-gas atom/surface interactions is determined by a balance between the exchange-repulsion and the attractive long-range dispersion contributions. The dispersionless interaction is clearly less repulsive when the Xe atom is located on top of the five-fold coordinated Ti_{5f} atom while the dispersion contribution is larger on top of the same site. Notice that the adsorption energy differences between the Ti_{5f} and O_{brid} positions become more pronounced when the dispersion correction is included. On one hand, since the static polarizability is larger for the O^{2-} ion than for the Ti^{4+} cation in TiO_2,[8] the dispersion interaction is more attractive for the Xe$-$O pair than for the Xe$-$Ti counterpart. On the other hand, when the Xe atom is located on top of the Ti_{5f} atom, it benefits from the dispersion interaction with bridging oxygen atoms located at both sides of the Ti_{5f} atom. Therefore, the clear preferential adsorption of the Xe atom on top of the Ti_{5f} site can be easily understood, as in previous studies of the He-TiO_2(110) interaction (see, e.g., Refs. 9,10).

As can be seen in Figure S2, the open-shell Ag/TiO_2(110) interaction differs greatly from the closed-shell Xe/TiO_2(110) interaction. In contrast with the latter, the vdW-uncorrected (disper-

sionless) Ag/TiO_2(110) interaction is already significantly attractive and this attractive interaction becomes favored on top of the O_{brid} site. This feature reflects the tendency of silver atoms with an unpaired electron to donate part of its electronic charge to the under-coordinated O^- anion in the TiO_2 surface and being strongly polarized. As shown for the Ag_2/TiO_2(110) interaction from a Symmetry-Adapted Perturbation Theory (SAPT)-based decomposition (see Table 1 of the main text), the magnitude of the induction and dispersion terms at the potential minimum is very similar to each other. For the closed-shell Ag_2/TiO_2 system, with the Ag−Ag axis oriented perpendicularly to the surface plane, the induction contribution is expected to arise from the strong polarization of the Ag_2 electronic density upon approaching the material. However, charge-transfer energy contributions are also embedded into the SAPT-based induction energy,[11] being expected to play an important role in the case of the open-shell Ag/TiO_2(110) interaction.

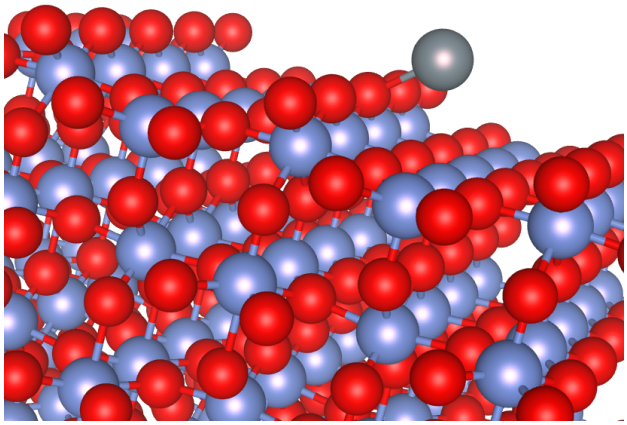

Figure S3: Structure of the Ag/TiO_2(110) system with the Ag atom located on top of a “hollow" site.

Interestingly, the adsorption energy differences for the Ag atom on top of the Ti_{5f} and O_{brid} sites become reduced when the dispersion D3(BJ) correction is added while the opposite holds for the Xe/TiO_2(110) interaction (see Figure S2). For the Ag/TiO_2(110) case, it reflects the competition between dispersion and additional attractive (dispersionless) energy contributions. The dispersion energy is larger on top of the Ti_{5f} atom for the same reason as for the Xe/TiO_2(110)

system: this symmetric position allows the Ag atom to benefit from the long-range dispersion interaction with bridging oxygen anions at both sites of the Ti_{5f} atom. On the other hand (see above), the attractive polarization and charge-transfer contributions are favored on top of the bridging oxygen atom. It should be stressed, however, that our analysis has been restricted to the Ti_{5f} and O_b adsorption sites. Thus, the adsorption on the hollow site shown in Figure S3 is more attractive by 70 meV, with the adsorption energy being -1009 meV. Hollow sites have been reported as most favored positions for the Ag/TiO_2 (anatase) and $Au/TiO_2(110)$ systems.[12,13]

S3 Complementary results on the $Ag_2/TiO_2(110)$ interaction

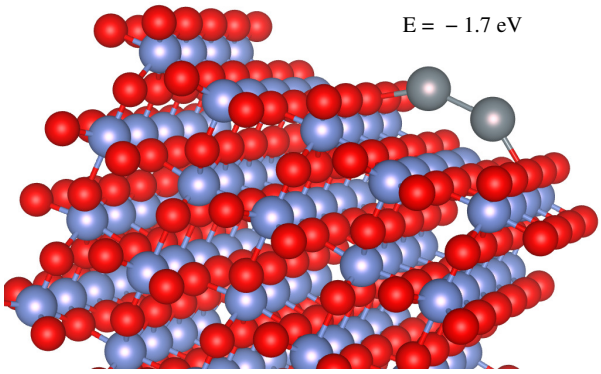

Figure S4: Optimized geometry and binding energy of the Ag_2 cluster upon adsorption on the $TiO_2(110)$ surface. Gray spheres represent silver atoms while red and blue spheres stand for oxygen and titanium atoms.

As for the Ag_3 and Ag_5 clusters (see main manuscript), the geometry of the supported Ag_2 cluster was relaxed starting with that optimized for the separated Ag_2 dimer using the PBE-D3(BJ) approach (see Table S1). Upon adsorption, the internuclear Ag−Ag distance becomes ca. 0.04 Å larger (from 2.56 to 2.60 Å). As can be seen in Figure S4, the Ag−Ag internuclear axis of the optimized structured become oriented perpendicularly to the Ti_{5f} row, with the Ag_2 center-of-mass being on top of the Ti_{5f} atom. Assuming a van-der-Waals(vdW)-dominated interaction, the favored rotation from the structure with the Ag−Ag internuclear axis oriented in a parallel configuration to the Ti_{5f} row (see Figure 2 of the main manuscript) to that presented in Figure S4

can be understood by considering that it makes the Ag-O_{brid} distances shorter and, then, the net Ag-O_{brid} dispersion contribution larger. However, besides the dispersion, additional attractive contributions are important in stabilizing the Ag-O_{brid} bonds (see bellow).

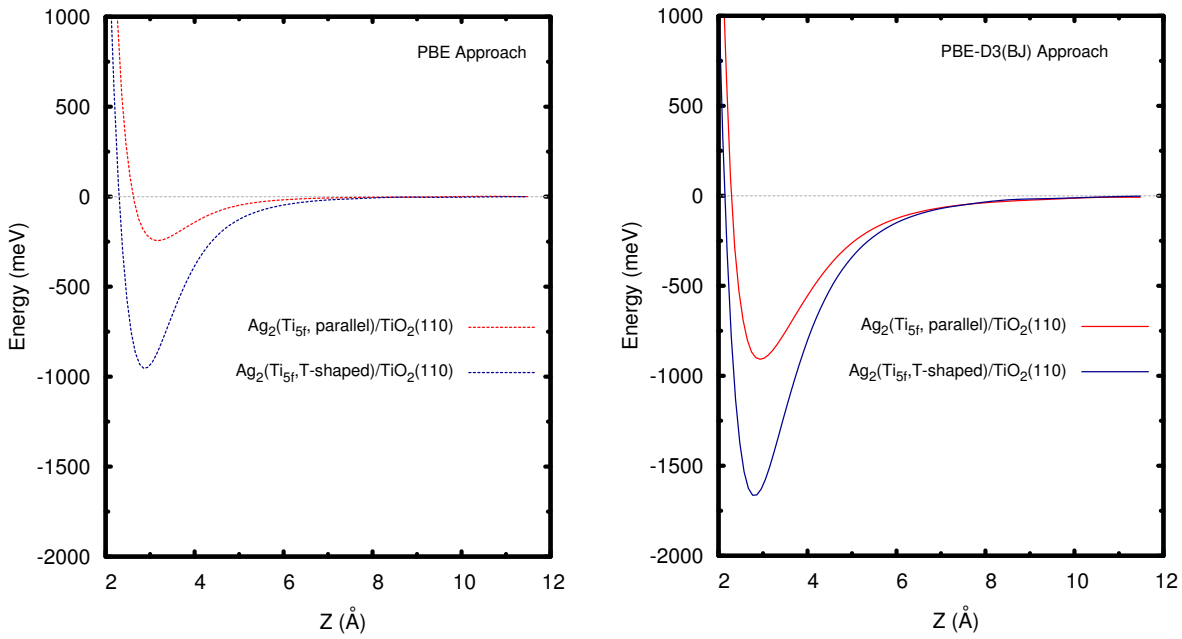

Figure S5: Radial scan of the interaction energies between the Ag_2 dimer and the TiO_2(110) surface, as calculated with PBE method (left-hand panel) and the vdW-corrected PBE-D3(BJ) scheme (right-hand panel). The cluster center-of-mass is located on top of the five-fold titanium atom Ti_{5f} (Ti_{5f} site) Z stands for the distance between the dimer center-of-mass and the Ti_{5f} atom along the surface normal direction. For the “T-shaped" configuration adsorption sites, the internuclear Ag−Ag axis is perpendicular to the direction of the row of Ti_{5f} atoms while the opposite holds for the “parallel" arrangement.

By keeping the internuclear Ag−Ag distance fixed to the experimentally determined value of 2.531 Å, Figure S5 compares the Ag_2/TiO_2(110) interaction potentials for the “T-shaped" configuration (i.e., with the Ag−Ag internuclear axis oriented perpendicularly to the Ti_{5f} row) and the “parallel" approach (i.e., with the the Ag−Ag internuclear axis being collinear to the Ti_{5f} row). It can be observed that the inclusion of the dispersion correction stabilizes very similarly both configurations. However, the uncorrected-vdW interaction is already much more attractive for the “T-shaped" approach. It indicates the partial covalent nature of the Ag-O_{brid} bond in that configu-

ration. Contrarily, for the “parallel" approach, the bonding is mainly determined by non-covalent vdW-type contributions.

References

(1) Weigend, F.; Ahlrichs, R. Balanced Basis Sets of Split Valence, Triple Zeta Valence and Quadruple Zeta Valence Quality for H to Rn: Design and Assessment of Accuracy. *Phys. Chem. Chem. Phys.* **2005**, *7*, 3297–3305.

(2) Neese, F. Software Update: the ORCA Program System, Version 4.0. *Wiley Interdisciplinary Reviews: Computational Molecular Science* **2018**, *8*, e1327.

(3) Haslett, T. L.; Bosnick, K. A.; Moskovits, M. Ag_5 is a Planar Trapezoidal Molecule. *J. Chem. Phys.* **1998**, *108*, 3453–3457.

(4) Simard, B.; Hackett, P. A.; James, A. M.; Langridge-Smith, P. R. R. The Bond Length of Silver Dimer. *Chem. Phys. Lett.* **1991**, *186*, 415–422.

(5) Monkhorst, H. J.; Pack, J. D. Special Points for Brillouin-Zone Integration. *Phys. Rev. B* **1976**, *13*, 5188–5192.

(6) de Lara-Castells, M. P.; Bartolomei, M.; Mitrushchenkov, A. O.; Stoll, H. Transferability and Accuracy by Combining Dispersionless Density Functional and Incremental Post-Hartree-Fock Theories: Noble gases Adsorption on Coronene/Graphene/Graphite Surfaces. *J. Chem. Phys.* **2015**, *143*, 194701.

(7) Tamijani, A. A.; Salam, A.; de Lara-Castells, M. P. Adsorption of Noble-Gas Atoms on the TiO_2(110) Surface: An Ab Initio-Assisted Study with van der Waals-Corrected DFT. *J. Phys. Chem. C* **2016**, *120*, 18126–18139.

(8) Dimitrov, V.; Sakka, S. Electronic Oxide Polarizability and Optical Basicity of Simple Oxides. I. *J. Appl. Phys.* **1996**, *79*, 1736–1740.

(9) de Lara-Castells, M. P.; Aguirre, N. F.; Mitrushchenkov, A. O. Physisorption of Helium on a TiO_2(110) Surface: Periodic and Finite Cluster Approaches. *Chem. Phys.* **2012**, *399*, 272–280.

(10) Aguirre, N. F.; Mateo, D.; Mitrushchenkov, A. O.; Pi, M.; de Lara-Castells, M. P. Helium-Mediated Deposition: Modeling the He-TiO_2(110)-(1$\times$1) Interaction Potential and Application to the Collision of a Helium Droplet from Density Functional Calculations. *J. Chem. Phys.* **2012**, *136*, 124703.

(11) Stone, A. J.; Misquitta, A. J. Charge-transfer in Symmetry-Adapted Perturbation Theory. *Chem. Phys. Lett.* **2009**, *473*, 201–205.

(12) Puigdollers, A. R.; Schlexer, P.; Pacchioni, G. Gold and Silver Clusters on TiO_2 and ZrO_2 (101) Surfaces: Role of Dispersion Forces. *J. Phys. Chem. C* **2015**, *119*, 15381–15389.

(13) de Lara-Castells, M. P.; Aguirre, N. F.; Stoll, H.; Mitrushchenkov, A. O.; Mateo, D.; Pi, M. Communication: Unraveling the ^{4}He Droplet-mediated Soft-landing from Ab initio-Assisted and Time-Resolved Density Functional Simulations: Au@$^4He_{300}$/TiO_2(110). *J. Chem. Phys.* **2015**, *142*, 131101.